Temperature dependence of crack-propagation parameters and crack morphology of the semicrystalline polyester poly(1,4-dimethylene-*trans*-cyclohexyl suberate)

J. M. Pochan, J. F. Elman and W. F. Parsons
Research Laboratories, Eastman Kodak Company, Rochester, NY 14650, USA
(Received 20 May 1983)

Temperature-dependent crack propagation in the semicrystalline polymer poly(1,4-dimethylene-*trans*-cyclohexyl suberate) was studied as a function of forming temperature (spherulitic morphology) and molecular weight. All experiments were conducted between the glass transition temperature and the crystal melting point. Higher forming temperature (larger spherulitic size) produced lower energy to propagate (G_p). For a given morphology (single forming temperature), increasing the propagation temperature decreased the propagation energy. An equation relating G_p to the microscopic viscosity of the amorphous polymer fraction was derived. Experimental data were fitted to the equation, and Arrhenius activation energies for microscopic flow were obtained. The results show a decrease in activation energy with increased forming temperature and molecular weight, and are discussed in terms of lamellar tie-molecule population. Fracture morphology is related to thermal parameters and chain entanglements. The results indicate that much of G_p is due to plastic deformation.

(Keywords: crack; propagation; polymer; semicrystalline; temperature dependence; morphology)

INTRODUCTION

The study of fracture in polymers has become increasingly important with their increased use as engineering materials[1-3]. These studies can be particularly relevant with semicrystalline polymers where crystallinity, spherulitic size and lamellar thickness can affect the fracture of the material. Early work on polypropylene showed that K_c (critical stress intensity factor) decreased linearly with spherulitic diameter, increased with strain rate and increased with molecular weight[4]. Within a given morphology, specific resistance to crack propagation could be attributed to regions with different morphological structure[5]. This meant that crazes could form in materials with small spherulitic morphology, whereas materials with very large spherulities fractured either inter- or intra-spherulitically[5]. Friedrich[6] further postulated a critical crack extension force G_c, which was a function of volume content of amorphous and crystalline material and their respective sizes and orientations.

The elastic properties of semicrystalline materials are also a function of the morphological character of the polymer. Patel and Phillips[7] correlated the Young's modulus (E) of high-density polyethylene (PE) with the spherulitic radius of the crystallites. Later, McCready *et al.*[8] showed that lamellae and polymer tie molecules between lamellae could affect the mechanical properties of PE.

In our paper concerning crack propagation in the semicrystalline polymer poly(1,4-dimethylene-*trans*-cyclohexyl suberate) (MCS) (see *Figure 1*)[9] we showed that the energy to propagate a crack (G_p) in MCS was dependent upon the spherulitic radius to the $\frac{1}{2}$ power. Such dependence is predicted when a modified Griffith criterion[10] is applied to micro-crystalline ceramic materials[11-13] and suggests that inter-spherulitic boundaries are important in the failure mechanism in MCS. Annealing studies on MCS[9], however, suggested that lamellar thickness may be more appropriate in describing the failure criterion. Recent small-angle X-ray scattering (SAXS) measurements have verified the former[9].

In the aforementioned studies, temperature was used only to produce the different morphologies in the polymers studied. No studies of the effect of temperature on fracture have been reported. We thus undertook an investigation of the effect of experimental temperature on crack propagation in MCS.

EXPERIMENTAL

Materials

Two samples of MCS were synthesized for use in these studies. They are designated MCS-I ($\bar{M}_n = 25\,000$, $\bar{M}_w = 48\,000$) and MCS-II ($\bar{M}_n = 38\,000$, $\bar{M}_w = 77\,500$). Both had molecular weights above the entanglement M_c of the polymer[9].

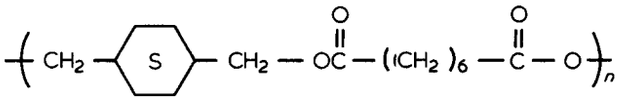

Figure 1 Structure of poly(1,4-dimethylene-*trans*-cyclohexyl suberate)

0032-3861/84/071040-09$03.00

Sample preparation

Crack propagation samples were prepared in Teflon moulds $10 \times 1 \times 0.32$ cm^3. MCS was melted into the moulds at 413K. The samples were then quenched in a water bath at the desired annealing temperature. The quenched samples were transferred to an oven at the same temperature and annealed for 21 h. Cracks were placed in the sample either by a razor-blade notch or by inserting a piece of 75 μm Teflon-coated Kapton into the sample during the forming phase. A 0.5 cm crack was used in all samples.

Mechanical testing

Crack propagation was studied on an Instron model 1113 instrument. Samples were held in pneumatic grips and tested in the tensile mode. The gauge length for all samples was 4.5 cm. The crack tip was observed with a Gaertner optical extensometer, and propagation was noted visually. The crosshead rate for these experiments was 0.2 cm min^{-1}.

Samples run at high temperatures were equilibrated for ~20 min before crack propagation. The sample was assumed to be at equilibrium when no forces developed in the Instron due to thermal expansion of the sample. Within the 20 min equilibration, lamellar thickness is not expected to vary significantly for those samples formed at low temperature and tested at higher temperature[14]. Three sample formation temperatures were used for each MCS sample. MCS-I samples were prepared at 30°, 65° and 90°C. These temperatures were chosen because ambient-temperature crack-propagation studies[9] showed significant differences in the crack-propagation parameters (energy to propagate, etc.) over this temperature range. For MCS-II, 50°, 70° and 90°C were chosen because samples prepared at lower temperatures did not propagate cracks well and in most cases necked. These temperatures provided light-scattering average spherulitic radii of 6, 30 and ~500 μm for MCS-I and 9, 18 and ~200 μm for MCS-II. Mechanical data such as energy to break were calculated in the standard fashion.

Physical characterization

Physical characterization of the polymers was reported earlier[9]. Polymer crystallinity for MCS-I and MCS-II as determined via d.s.c. varied slightly with temperature of formation from the melt but could be considered constant at $45 \pm 3\%$ over the experimental temperature range. This suggests little effect of degree of crystallinity on the observed mechanical properties of the polymer[15]. Annealing has shown little effect on the degree of crystallinity of MCS. T_m for MCS-I was $97.4° \pm 0.8$°C for all samples formed and annealed below 90°C and increased to 104°C for samples formed above this temperature. The latter indicates a lamellar thickening in this region[16]. For MCS-II T_m was $96.8° \pm 1.2$°C for all samples. Room-temperature elastic moduli were 362 ± 20 MPa for MCS-I and 370 ± 33 MPa for MCS-II for formation temperatures 8° to 75°C below T_m. Spherulitic size varied continuously from ~4 μm (20°C) to 400 μm (90°C) for MCS-I and from 3 μm to ~200 μm for MCS-II in the same temperature regime. Both samples show banding morphology in this region, with an abrupt change in banding character appearing above 85°C[9]. T_g for MCS is −20°C.

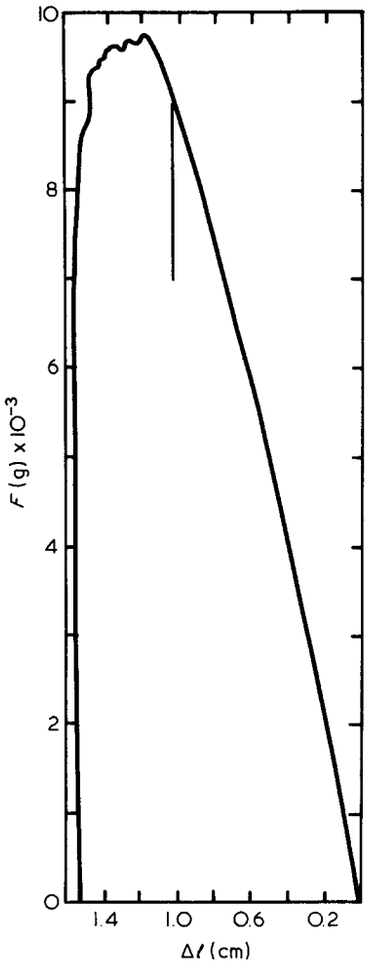

Figure 2 Force vs. displacement for a sample of MCS-I at 60°C. Event mark is propagation point

RESULTS AND DISCUSSION

Crack propagation parameters

Figure 2 shows results of a typical crack-propagation run. Propagation occurs immediately after deviation from the elastic region of the material. This failure mode was common in all samples, and a plot of energy to propagate (G_p) vs. $E\varepsilon_p^2$ for all samples (see *Figure 3*) shows that the materials behaved almost totally elastically until propagation. In the above, E is Young's modulus and ε_p is the strain at propagation. This result is interesting in that, within the temperature range studied, micrographs show various degrees of plastic deformation during fracture (see below). The result may indicate that microscopic propagation occurs during the elastic region of deformation but that the crack does not become visible until much larger-scale deformation of the sample occurs.

The temperature dependences of Young's modulus for both polymers as a function of sample-formation temperature and crack-propagation temperature are shown in *Figures 4* and *5*. Within experimental error the log E values are linearly related to temperature for MCS-I over the entire experimental region. The values for MCS-II are again logarithmically related to temperature up to ~70°C. Above this temperature the modulus drops off drastically. These data are not unlike those observed for other crystalline polymers[17] in the temperature regime between T_g and T_m. The abrupt downturn in E near T_m for MCS-II vs. MCS-I suggests a more highly perfected

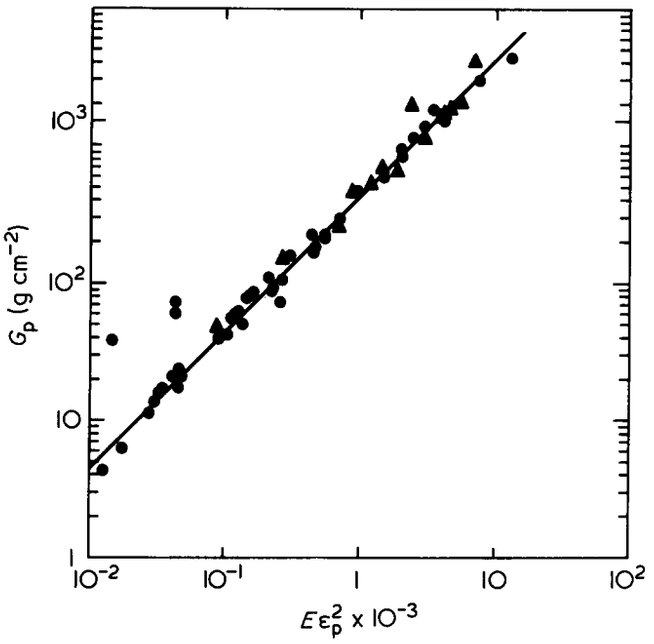

Figure 3 Energy to propagate vs. $E\varepsilon_p^2$ for all samples of MCS-I and MCS-II studied

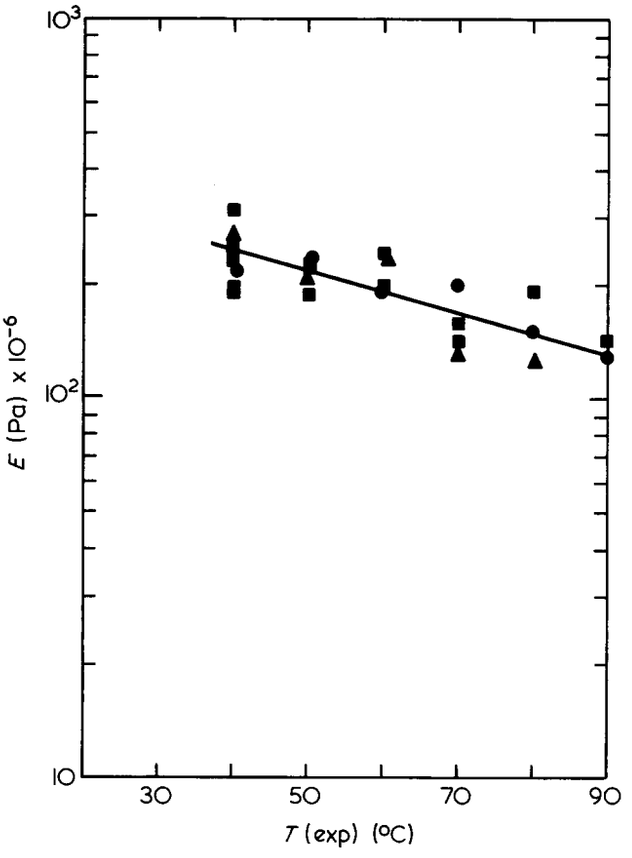

Figure 4 Tensile modulus vs. experimental temperature for MCS-I. Annealing temperature: (▲) 30°C; (■) 65°C: (●) 90°C

crystalline structure in MCS-I, thus fewer premelt phenomena and less loss of strength[18]. The higher E for MCS-II compared to MCS-I is not unexpected, as spherulitic size and most probably lamellar thickness are smaller[7,8].

The energy to propagate (G_p) for both polymers as a function of experimental temperature is shown in *Figures 6* and *7*. The data indicate large changes in G_p with temperature, with MCS-I being linear on a log G_p vs. T plot and MCS-II having G_p values that decrease gradually with increasing temperature and then drop much faster at temperatures >60°C. This is in sharp contrast to the slowly varying modulus data.

Temperature dependence

The temperature dependence of G_p for the above data can be fitted with the following equation:

$$G_p = \frac{1}{C_1} + \frac{1}{C_2 \exp(-E_a/RT)} \tag{1}$$

Although equation (1) is a three-parameter equation, C_1 and C_2 are defined by boundary conditions and the value of E_a (the activation energy). For instance, at T_m, $G_p = 0$ as the polymer becomes liquid and will not propagate a crack. Therefore,

$$C_1 = -C_2 \exp(-E_a/kT_m) \tag{2}$$

and equation (1) becomes

$$G_p = \frac{1}{C_2}\left(\frac{1}{\exp(-E_a/kT)} - \frac{1}{\exp(-E_a/kT_m)}\right) \tag{3}$$

C_2 can then be determined by any other data point in the experimental set. In our evaluation, this point was usually chosen at $T_m - T$ a maximum for a given set. If this temperature is defined as T_r, then equation (3) becomes

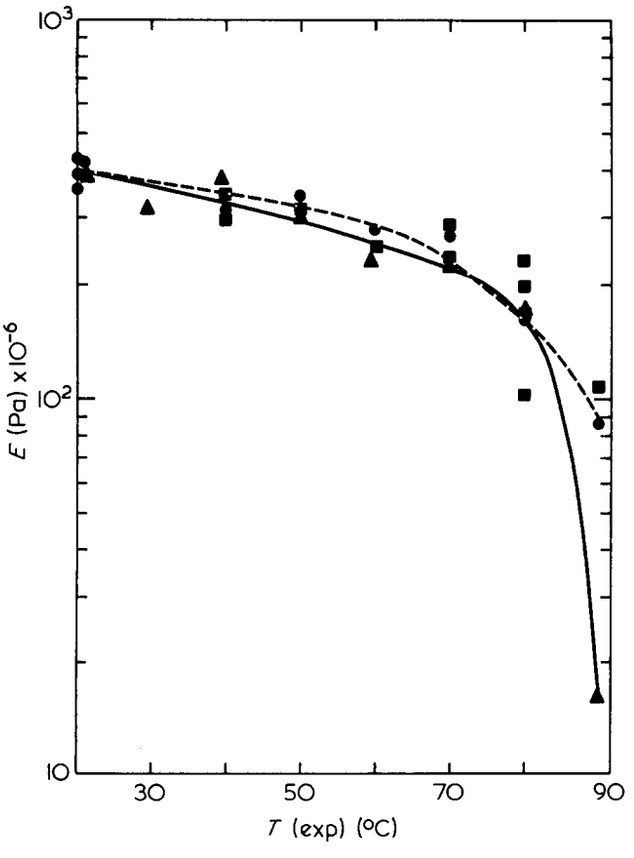

Figure 5 Tensile modulus vs. experimental temperature for MCS-II. Annealing temperature: (▲) 50°C; (■) 70°C; (●) 90°C

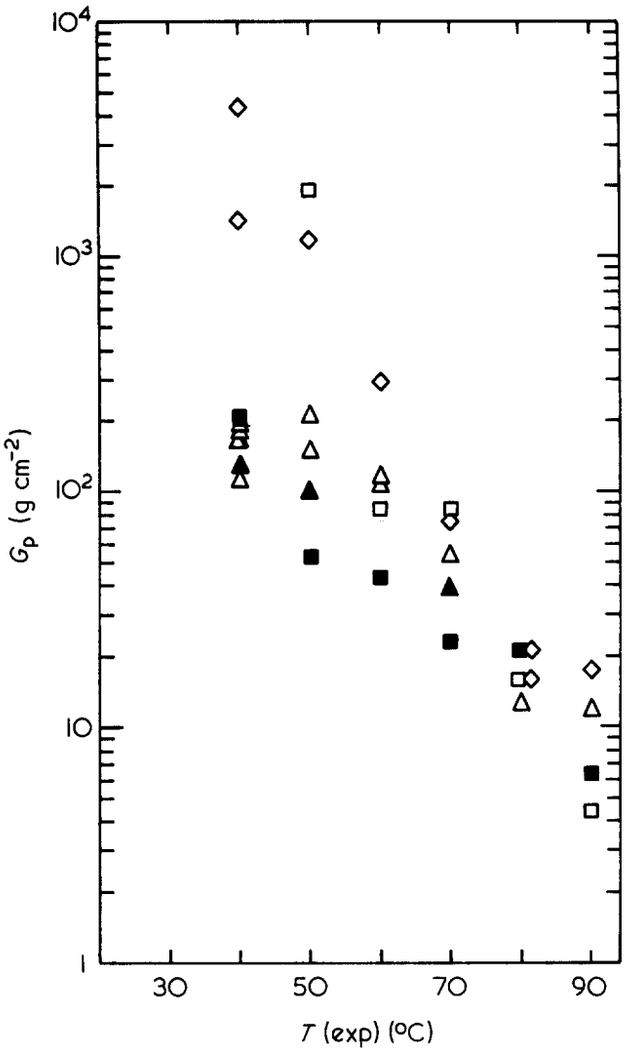

Figure 6 Energy to propagate vs. experimental temperature for MCS-I. Annealing temperature: (◇) 30°C; (△, ▲) 65°C; (□, ■) 90°C

$$G_{p(T_r)} = \frac{1}{C_2}\left(\frac{1}{\exp(-E_a/kT_r)} - \frac{1}{\exp(-E_a/kT_r)}\right) \quad (4)$$

and C_2 can be calculated. G_p thus becomes a function of E_a only with these conditions. *Figures 8* and *9* show a fit of G_p data for MCS-I and MCS-II; the experimental data can be reproduced quite well.

Equation (1) is a generalized equation with the value of C_2 determining the absolute level of G_p. Because of this, a reduced plot of G_p vs. T can be generated as a function of activation energy. This plot can then overlay the data to obtain a best fit. The reduced plot is shown in *Figure 10*, where the curvature at temperatures near T_m is effectively eliminated as E_a is increased.

Rationale for equation (1)

The energy to propagate in a completely elastic material is given by $E\varepsilon^2/2$. On a macroscopic scale it has been shown that MCS exhibits little temperature dependence of the modulus and all temperature dependence for G_p would be contained in ε. We believe, however, that localized conditions in the crack tip region must be considered for propagation and that, when this is done, the temperature dependence of E and ε must be considered.

The amorphous material in MCS is above T_g in these experiments and, as such, should react to the applied extensive force as a crosslinked material, the crosslinks being the lamellae of MCS. When stress is initially applied, the material will react on a microscale by first stretching any tie molecules between lamellae. During this time, if the chains have a sufficienty short relaxation time, a general reorganization of the amorphous material can take place. If the relaxation time is long with respect to the experimental time frame, the matrix will tend to distort with reorganization, until the amorphous material is in an extended lower entropy state than it was initially. At this point, two things can happen, bond breaking of the extended chain or reorganization of the crystalline regions[19-23]. In the latter case, plastic deformation and necking of the polymer occur. This has been observed for MCS-II propagated at room temperature and to some extent in certain regions of band orientation during transspherulitic fracture (see below), but it probably does not occur in brittle fracture regions. It would thus appear that the energy required to initiate propagation is distributed between a true deformation process (viscous flow of the amorphous regions) and the breaking of tie molecules or fracture of the lamellar structure.

To a first approximation, the energy required to

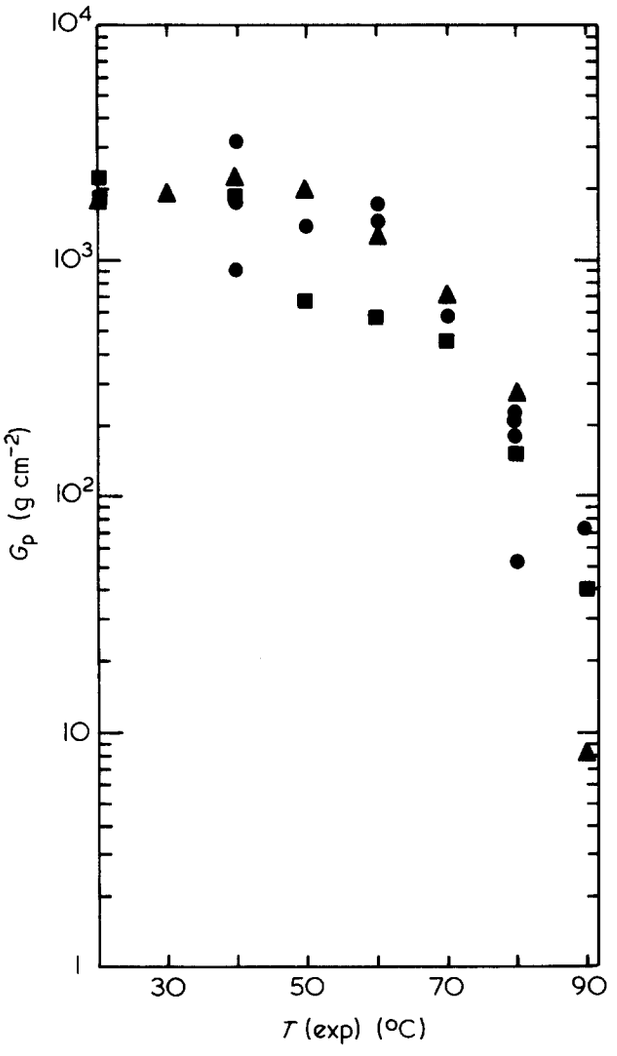

Figure 7 Energy to propagate vs. experimental temperature for MCS-II. Annealing temperature: (▲) 50°C; (●) 70°C; (■) 90°C

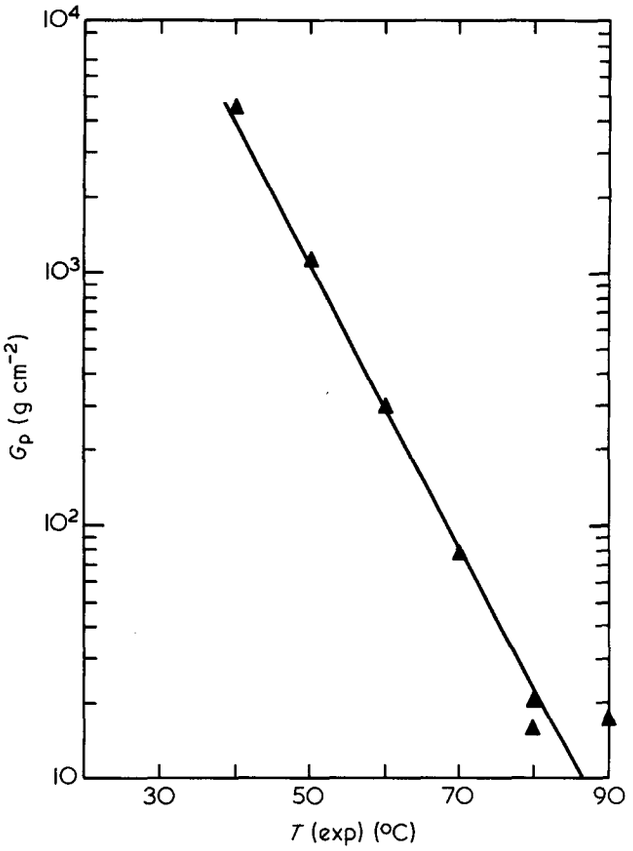

Figure 8 Energy to propagate vs. experimental temperature for an MCS-I sample prepared and annealed at 30°C; (▲) experimental data; (—) theoretical fit with E_a=27 kcal mol^{-1}

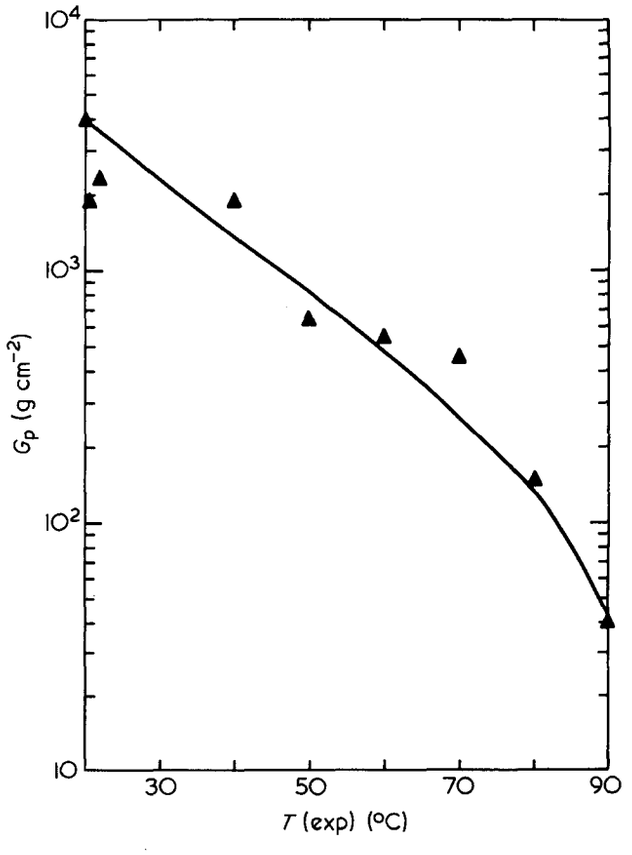

Figure 9 Energy to propagate vs. experimental temperature for an MCS-II sample prepared and annealed at 50°C; (▲) experimental data; (—) theoretical fit with E_a=9 kcal mol^{-1}

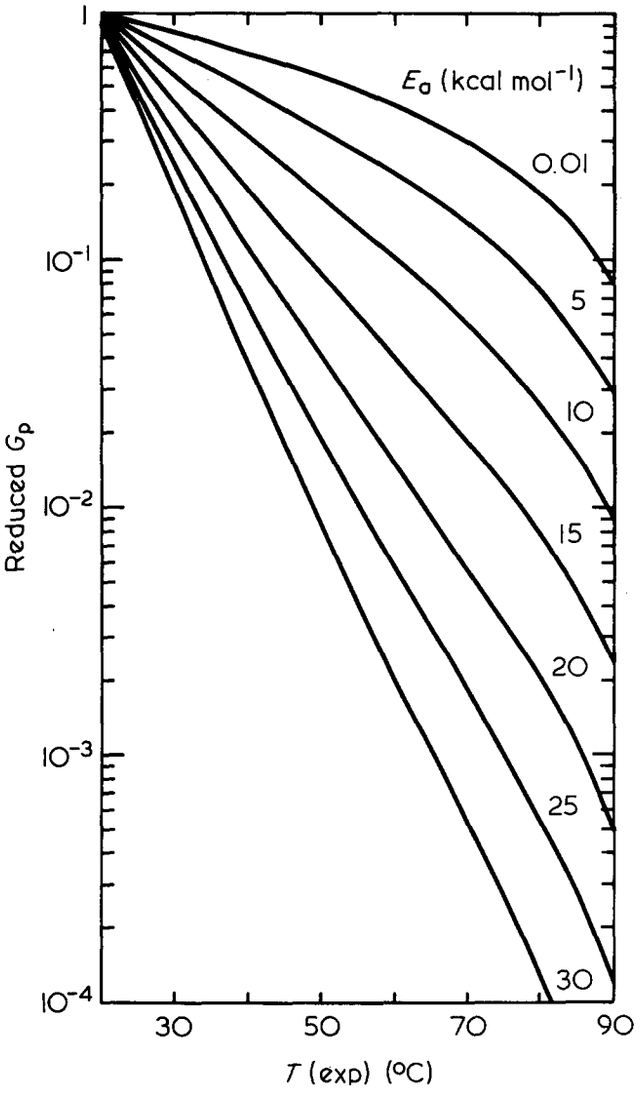

Figure 10 Reduced energy to propagate vs. temperature as a function of activation energy

propagate would be the sum of two terms, the elastic energy and the energy required to break tie molecules during deformation. The latter effect has been discussed extensively for crosslinked rubbers[20,21]. For a given annealing and crystallization temperature, this bond-breaking term should be constant as a function of temperature, whereas the first term would be temperature dependent. G_p can therefore be written

$$G_p = \tfrac{1}{2}E\varepsilon^2 + C_1 \tag{5}$$

The temperature dependence of E and ε can be derived qualitatively in the following way. The absolute strain in the material at the crack tip should be inversely proportional to the microviscosity of the amorphous material; the higher the temperature above T_g, the more readily the amorphous segments can respond to applied stress. G_p can therefore be written

$$G_p \simeq \frac{C_2' E}{\eta^2} + C_1 \tag{6}$$

The effective modulus at the crack tip can also be considered a function of the amorphous segment

viscosity; i.e. at lower viscosities E would be expected to be small, owing to the relaxational response of the amorphous segments until they are stretched to their final extension. G_p can therefore be written

$$G_p \simeq \frac{C_2\eta}{\eta^2} + C_1 = \frac{C_2}{\eta} + C_1 \quad (7)$$

The temperature dependence of η can now be included in equation (6) or (7). The temperature dependence of viscosity of purely amorphous polymer systems above T_g has been well characterized[22]. For temperatures well above T_g, η is Arrhenius activated, but nearer T_g, a WLF formalism is needed. Obviously, the use of the Arrhenius equation in equations (6) and (7) will produce equation (1). The empirical fit of the data can thus be qualitatively derived. The use of equation (6) or (7) to fit the data will, however, produce activation energies differing by a factor of 2.

Table 2 lists the activation energies determined by curve fitting the G_p data to equation (7) as described above. For MCS-II, G_p data were not fitted in the low-temperature region, where they were temperature independent. Equation (1) in this case predicted much higher values for G_p (by a factor of 2) than was observed. The low-temperature region will be discussed later. The error in E_a from the fit is estimated at ± 3 kcal mol^{-1}.

The E_a's for MCS-I and MCS-II are a factor of 2 different at similar annealing temperatures, with the higher-molecular-weight material giving the lower activation energy. Both samples show a decrease in E_a with increased annealing temperatures. This latter effect can be rationalized in terms of the lamellar structure of the polymer. McCready and coworkers[8] have shown that crystallization and annealing of polyethylene increase lamellar thickness but do not change the amorphous layer thickness. This suggests that certain lamellae are growing at the expense of others and thus polymer chains must be reeled into the crystal structure. Thus the number of tie molecules between lamellae is reduced. At higher crystallization temperatures, crystal growth is slower and the above-mentioned effect is more pronounced. We have previously shown that MCS-II exhibits brittle fracture when annealed at high temperatures but undergoes necking when the sample is quenched from the melt to room temperature. As the crystallinity in both cases is almost identical, such behaviour would be ascribed only to spherulitic size or lamellar growth processes. In the light of annealing studies similar to those of McCready[8], the latter is favoured.

When a semicrystalline material is stressed, first reorientation and then disruption of the lamellae occur[23]. In the elastic region reorientation is the prevalent mode of deformation. During reorientation, as lamellae shift amorphous material must flow; for instance, if two lamellae move apart, the amorphous material must flow and fill the space created. This flow is a function of the viscosity of the material as well as interlamellar tie density. If the tie-molecule population is large, reorientation of the matrix will be concerted, and a high barrier to reorientation would be expected. When tie-molecule population is low, the lamellae can effectively move independently of one another, and the barrier to motion would decrease. The decrease in E_a as a function of annealing temperature calculated from equation (1) is thus not unexpected in the light of annealing studies on other semicrystalline materials.

Table 1 E_a of equation (1) determined by curve fitting G_p vs. T data

Sample	E_a (kcal mol^{-1})	Sample-forming temperature (°C)
MCS-I	27	30
MCS-I	12	65
MCS-I	10	90
MCS-II	9	50
MCS-II	5	70
MCS-II	5	90

The molecular-weight/activation-energy correlation is more difficult to understand. For a given forming temperature, the spherulitic size of higher-molecular-weight MCS is smaller than that of its low-molecular-weight counterpart. Lamellar thickness has, however, been shown to increase with molecular weight for a given recrystallization temperature[24]. This increase is relatively small for high-molecular-weight materials, and identical crystallinities for both materials would show a higher population of tie molecules in the high-molecular-weight material. On this basis and the argument given above, it would be expected that the activation energy measured for MCS-II would be higher than that of MCS-I. The fact that it is not may mean: (1) that the higher-molecular-weight lamellae are more easily reoriented, even with a higher tie-molecule population, than their low-molecular-weight counterpart or (2) that the two systems should not be compared because of changes in the deformation characteristics of MCS-II and MCS-I with temperature.

Equation (7) considers the reponse of the polymer on a microscale in the crack-tip region and, as such, may present a valid picture. Experimentally, however, the macroscopic strain to break (ε_p) decreases with increasing temperature for the variously annealed samples. This behaviour is unlike that for highly crosslinked rubbers, whose behaviour is qualitatively predicted from equations (6) and (7) and the assumptions made to derive them[25]. Such behaviour can be rationalized only by considering the microresponse of the crack tip and the macroresponse of the sample to be quite different. Energy density theories have shown that the strain energy density in the crack-tip region is significantly different from those observed on a macroscale[2].

Even through the macroresponse of MCS differs from the above qualitative prediction of temperature effects, we feel that equation (6) or (7) qualitatively describes microstructural events and their temperature dependences.

Fracture-morphology variation with temperature

The room-temperature fracture morphology of MCS has been discussed in terms of forming temperature[9]. The following addresses the fracture morphology as a function of experimental temperature and relates it to other semicrystalline systems that have been studied.

The forming temperatures produced spherulitic sizes that vary by almost two orders of magnitude for MCS-I and MCS-II. During each temperature experiment, it is expected that gross morphological structure will be little affected. The changes observed with temperature will thus be associated with thermal changes in the semicrystalline microstructure (see above). For a given forming tem-

perature, decreasing the expermental temperature increases the energy to propagate, and this is correlated with increased plastic deformation of the fracture surface (*Figures 11* and *12*). *Figure 12a* shows that at low temperatures cavitation occurs at the crack surface. There is little evidence of the spherulitic morphology of the system. In *Figure 11*, as the propagation temperature is increased, a transformation from plastic deformation to inter-spherulitic failure occurs. In *Figure 11a* (50°C), the distorted banded structure of the polymer is obvious, showing a morphological reorganization of the structure. In *Figure 11b* (70°C), plastic deformation is still seen, but now portions of spherulitic structure covered with

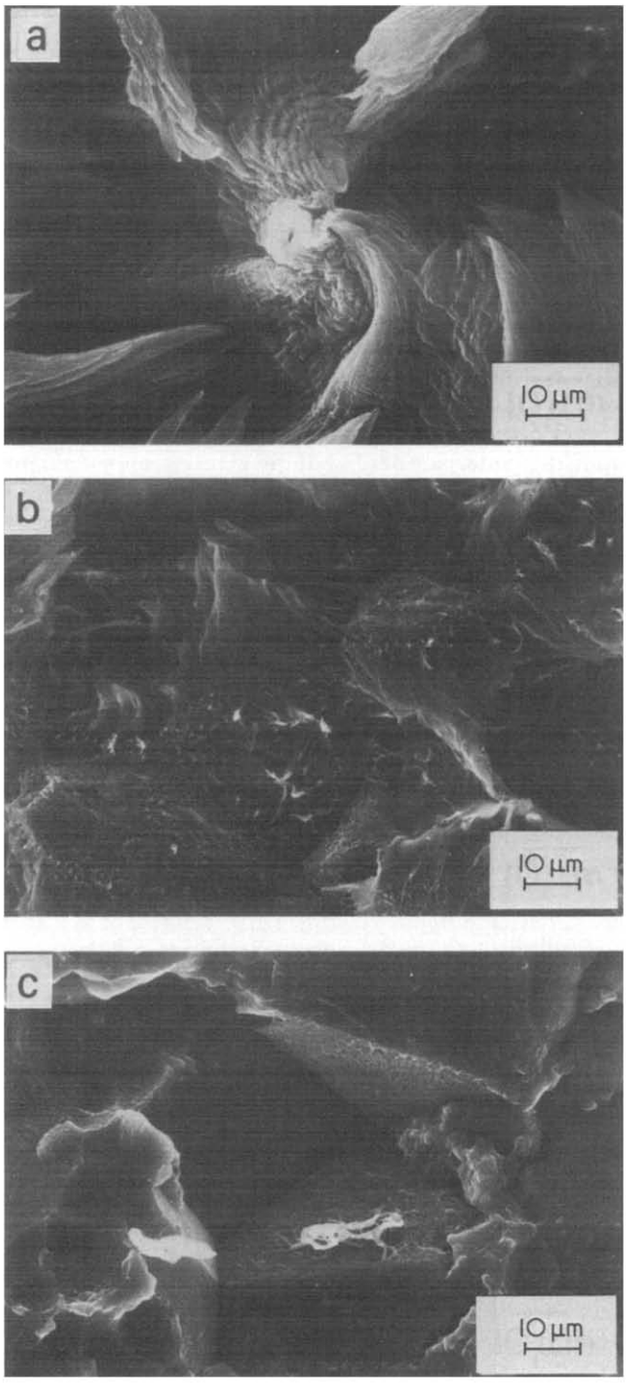

Figure 11 Fracture morphology for MCS-II as a function of temperature. Sample formed at 90°C. Experimental temperature: (a) 50°C; (b) 70°C; (c) 90°C

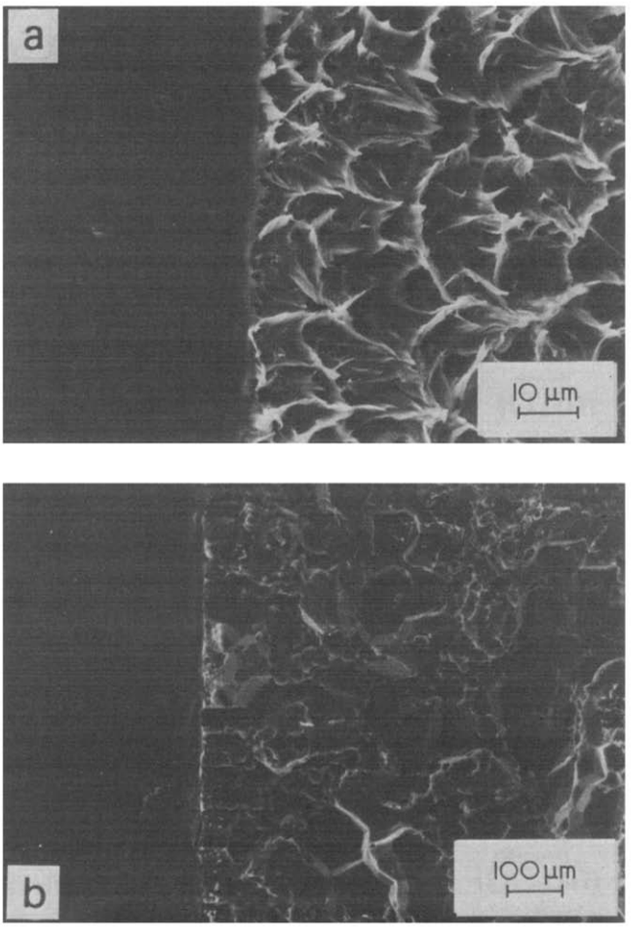

Figure 12 Fracture morphology for MCS-II at the crack-propagation front as a function of experimental temperature. Forming temperature for both samples is 90°C. Experimental temperature: (a) 40°C; (b) 90°C

plastically deformed MCS are observed. Finally, at 90°C inter-spherulitic fracture has occurred, with only slight indications of a plastically deformed material at the surface of any individual spherulite (*Figure 11c*). These morphologies indicate that G_p for this system is a function of the plastic deformation character, with higher energy required, as expected, for a more plastically deformed material. A lower magnification of the crack front is shown in *Figure 12* at the highest and lowest propagation temperatures; again, the failure mode proceeds from plastic deformation to inter-spherulitic failure.

Figure 12b also shows that propagation begins in a trans-crystalline front in the polymer. The fracture surface of a large spherulite shown in *Figure 13* for MCS-II shows plastically deformed material on the face of the fracture surface. Within the time frame of the experiment, these results for MCS-II show that during fracturing at high temperature, the molecular chains in the polymer respond to the implied stress and can slip past one another, permitting an inter-spherulitic fracture, whereas at lower temperatures, the relaxation time of the molecules is longer than that of the experiment. The inter-spherulitic tie molecules cannot relax, and plastic deformation of the sample occurs.

The morphological data for MCS-I are similar to those of MCS-II, but the 'plastic deformation' zone is shifted to lower temperature. This is expected in terms of tie-molecule populations and molecular weights of the two

systems[8]. *Figure 14* shows morphology data for MCS-I at conditions similar to those of *Figures 11–13*. Two noticeable differences between the morphologies are observed:

(1) At lower temperatures, plastic deformation is not large-scale but localized (*Figure 14a*). In this micrograph, trans-annular fracture has occurred, but localized plastic deformation coincides with the band dimension. These localized deformation zones probably coincide with lamellar orientation (long axis) parallel to the stress direction so that deformation and reorientation of the crystal axis can occur[23,26,27]. In the interband region, the chain axis is already parallel to the implied stress, and further deformation cannot occur and brittle fracture takes place.

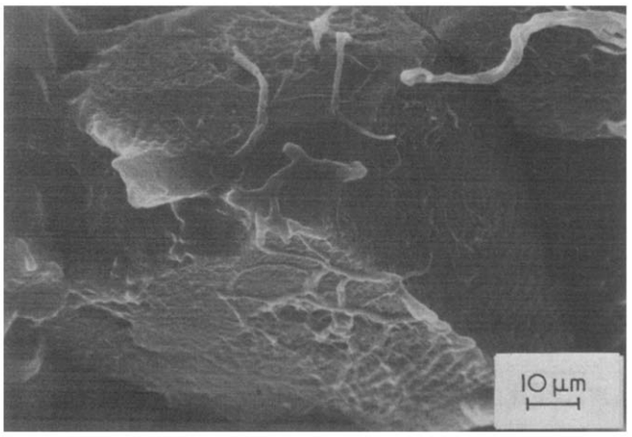

Figure 13 Fracture morphology for MCS-II. Forming temperature 90°C; propagation temperature 90°C

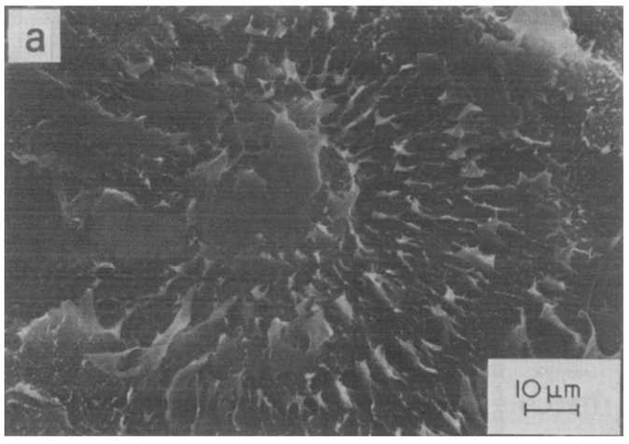

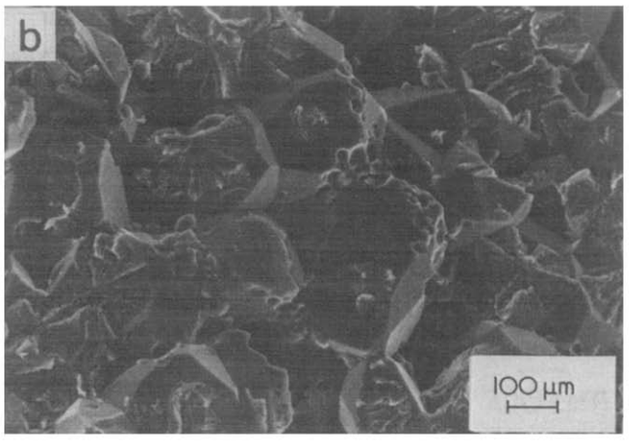

Figure 14 Fracture morphology for MCS-II. Forming temperature 90°C; propagation temperature: (a) 60°C; (b) 90°C

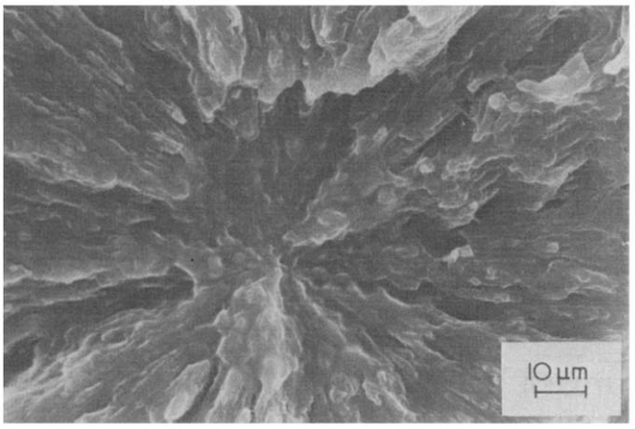

Figure 15 Fracture morphology for MCS-II in the trans-spherulitic fracture zone. Forming temperature 90°C; propagation temperature 90°C

(2) At higher propagation temperatures (*Figure 14b*), inter-spherulitic fracture takes place; however, this is interspersed with trans-spherulitic fracture. The latter was not observed in MCS-II. The trans-spherulitic fracture was observed by Friedrich in polypropylene[4].

The trans-spherulitic fracture was observed in fast-propagation zones of polypropylene. In MCS-I, these are observed at the propagation face and suggest fast propagation at high temperatures for MCS-I. A high magnification of a trans-spherulitic fracture (*Figure 15*) shows no plastic deformation at the fracture surface and a nodular structure. The cause of this nodular structure (nodules ~ 1–3 μm) is not known.

For MCS-I samples formed at lower temperatures, fracture behaviour parallels that of MCS-II. Representative morphologies are shown in *Figure 16*. At 60°C, plastic deformation is obvious, but not at the scale observed for MCS-II (see *Figure 12*). At 90°C, the fracture surface shows no apparent plastic deformation, and a 'rubberlike' appearance due to the smaller spherulitic size can be seen. A higher magnification of *Figure 16b* is shown in *Figure 17*, and plastic deformation is not obvious. These results again suggest that chain relaxation can be taking place within the time frame of the propagation experiment with concomitant changes in the mode of failure of the material. The results also suggest that the increased propagation energy is a function of the plastic deformation during crack propagation.

CONCLUSION

Temperature-dependent crack propagation in the semicrystalline polymer poly(1,4-dimethylene-*trans*-cyclohexyl suberate) was studied as a function of forming temperature (spherulitic morphology) and molecular weight. All experiments were conducted between the glass transition temperature and the crystal melting point. Higher forming temperature (larger spherulitic size) produced lower energy to propagate (G_p). For a given morphology (single forming temperature), increasing the propagation temperature decreased the propagation energy. An equation relating G_p to the microscopic viscosity

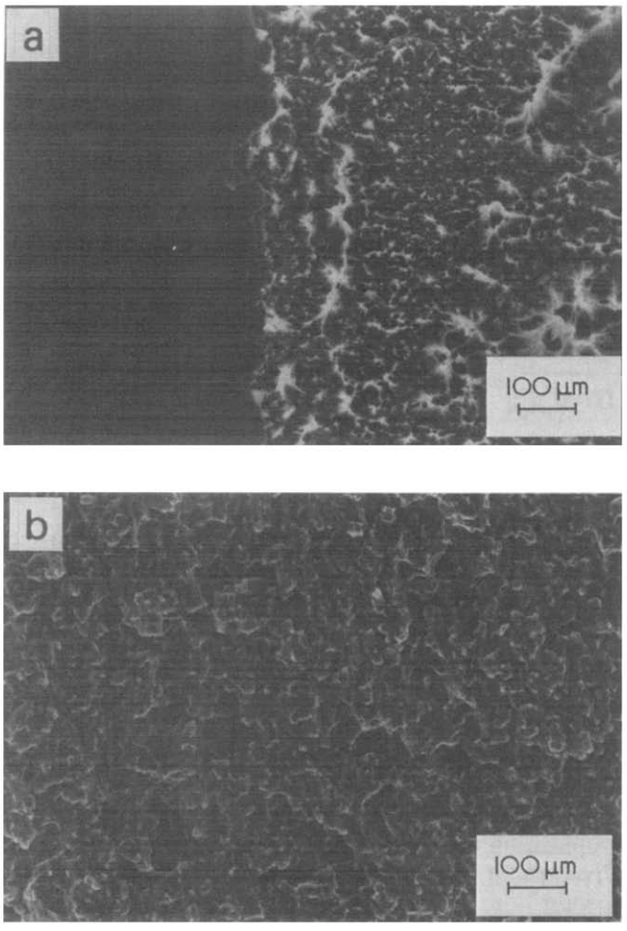

Figure 16 Fracture morphology for MCS-I. Forming temperature 30°C; propagation temperature: (a) 60°C; (b) 90°C

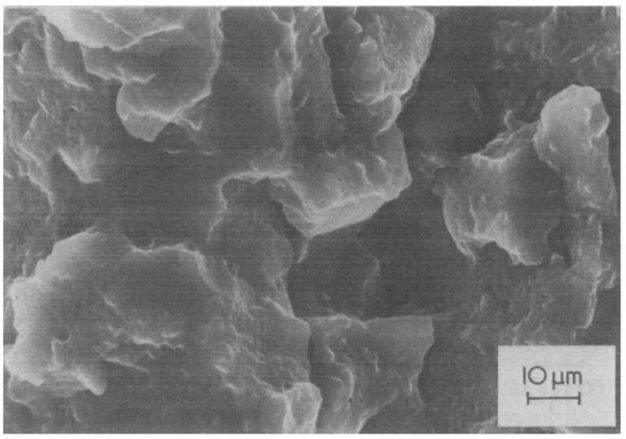

Figure 17 Fracture morphology for MCS-I. Forming temperature 30°C; propagation temperature 90°C

of the amorphous polymer fraction was derived. Experimental data were fitted to the equation, and Arrhenius activation energies for microscopic flow were obtained. The results show a decrease in activation energy with increased forming temperature and molecular weight, and were discussed in terms of lamellar tie-molecule population. Fracture morphology was related to thermal parameters and chain entanglements. The results indicate that much of G_p is due to plastic deformation.

ACKNOWLEDGEMENT

We thank Mr R. Gutierrez of the Kodak Industrial Laboratory for his excellent SEM work.

REFERENCES

1 Wu, S. 'Polymer Interface and Adhesion', Marcel Dekker, New York, 1982
2 Kausch, H. H. 'Polymer Fracture', Springer-Verlag, New York, 1978
3 Cherry, B. W. 'Polymer Surfaces', Cambridge University Press, New York, 1981
4 Friedrich, K. (Ed) 'Fracture', Vol. 3, ICF4, Waterloo, Canada, 1977
5 Wittkamp, I. and Friedrich, K. *Prakt. Metallogr.* 1978, **15**, 321
6 Friedrich, K. *Progr. Colloid Polym. Sci.* 1978, **64**, 103
7 Patel, J. and Phillips, P. J. *J. Polym. Sci., Polym. Lett. Edn.* 1973, **11**, 771
8 McCready, M. J., Schultz, J. M., Lin, J. S. and Hendrichs, R. W. *J. Polym. Sci., Polym. Phys. Edn.* 1979, **17**, 725
9 Pochan, J. M., Parsons, W. F. and Elman, J. F. *Polymer* 1984, **25**, 1031
10 Griffith, A. *Phil. Trans. R. Soc. Lond. A* 1921, **221**, 163
11 Rivlin, R. S. and Thomas, A. G. *J. Polym. Sci.* 1953, **10**, 291
12 Andrews, E. H. (Ed) 'Fracture in Polymers', Oliver and Boyd, London, 1968
13 Liebowitz, H. (Ed) 'Fracture', Academic Press, New York, 1972, p. 324 and references therein
14 Fischer, E. W. and Schmidt, G. F. *Angew. Chem. Int. Ed. Engl.* 1962, **1**, 488
15 Mohajer, Y. and Wilkes, G. L. *J. Polym. Sci., Polym. Phys. Edn.* 1982, **20**, 457
16 Bovey, F. and Winslow, F. (Eds) 'Macromolecules', Academic Press, New York, 1979, p 326
17 Deanon, R. P. 'Polymer Structure, Properties and Applications', Cahner, Boston, 1972, p 240
18 Baijal, M. D. (Ed) 'Thermal Characterization of Polymers' in 'Plastics Polymer Science and Technology', Wiley, New York, 1982, Chapter 5
19 Eshelby, J. D. *Proc. R. Soc. Lond., A* 1957, **241**, 376
20 Lake, G. J. and Thomas, A. G. *Proc. R. Soc. Lond., A* 1967, **300**, 108
21 Ref. 4, Chapter 8
22 Matsuoka, S. and Kwei, T. K. in 'Macromolecules' (Eds F. A. Bovey and F. M. Winslow), Academic Press, New York, 1979, Chapter 6
23 Samuels, R. J. in 'The Solid State of Polymers' (Eds P. Geil, E. Baer and Y. Wada), Wiley, New York, 1974, p 41
24 Mandelkern, L., Price, J. M., Gophan, M. and Fatou, J. G. *J. Polym. Sci. A* 1966, **4**, 385
25 Gent, A. N. and Petrich, R. P. *Proc. R. Soc. Lond. A* 1969, **310**, 433
26 Ingram, P. and Peterlin, A. *Encycl. Polym. Sci. Technol.* 1968, **9**, 204
27 Samuels, R. J. *J. Macromol. Sci. Phys. B* 1973, **8**, 41